Supplementary Information

RNA sequence and structure control assembly and function of RNA condensates

Raghav R. Poudyal[1,3,*], Jacob P. Sieg[1,3], Bede Portz[4], Christine D. Keating[1,*], Philip C. Bevilacqua[1,2,3,*]

[1]Department of Chemistry, [2]Department of Biochemistry, Microbiology, and Molecular Biology, [3]Center for RNA Molecular Biology, Pennsylvania State University, University Park, Pennsylvania, 16802, USA. [4] Department: Biochemistry and Biophysics, Perelman School of Medicine at the University of Pennsylvania, Philadelphia, PA 19104, USA.

*Authors to whom correspondence should be addressed

Prof. Philip C. Bevilacqua pcb5@psu.edu
Prof. Christine D. Keating keating@chem.psu.edu
Dr. Raghav R. Poudyal rup34@psu.edu

Contents **Page**

Supplementary text for thermal denaturation of riboswitches:

To investigate any undesired effects of mutations on RNA structure, we performed thermal melts of both WT and mutant of guanidine and guanine riboswitches. UV-thermal denaturation curves indicated that all riboswitches tested adopt several folding intermediates as indicated by multiple peaks in the first derivative plot (Supplementary Fig. S5). Overall, the similarity of melting curves for tested riboswitches and their respective mutants indicate that the mutations do not affect the stability of the core folded structure, supporting the conclusion that they function by increasing the potential for *trans* RNA-RNA interactions in a targeted fashion (Supplementary Text, Figs. 3 and 4). Briefly, all riboswitches and mutants show two transitions, albeit slightly attenuated for the UGGU (M1) mutation of the Gdn riboswitch.

	Nucleotide content (%)				Size (nt)	Free energy (kcal/mol)
	A	C	G	U		
Guanine	22.5	20.5	25.8	31.2	151	-47.8
Guanidine	29.0	18.9	29.1	23.0	148	-56.9
Ykkc_2c	21.9	16.6	27.2	34.3	169	-47.5

Supplementary Table 1: Nucleotide content in the guanine-, guanidine-, and Ykkc_2c-nucleotide-binding riboswitches.

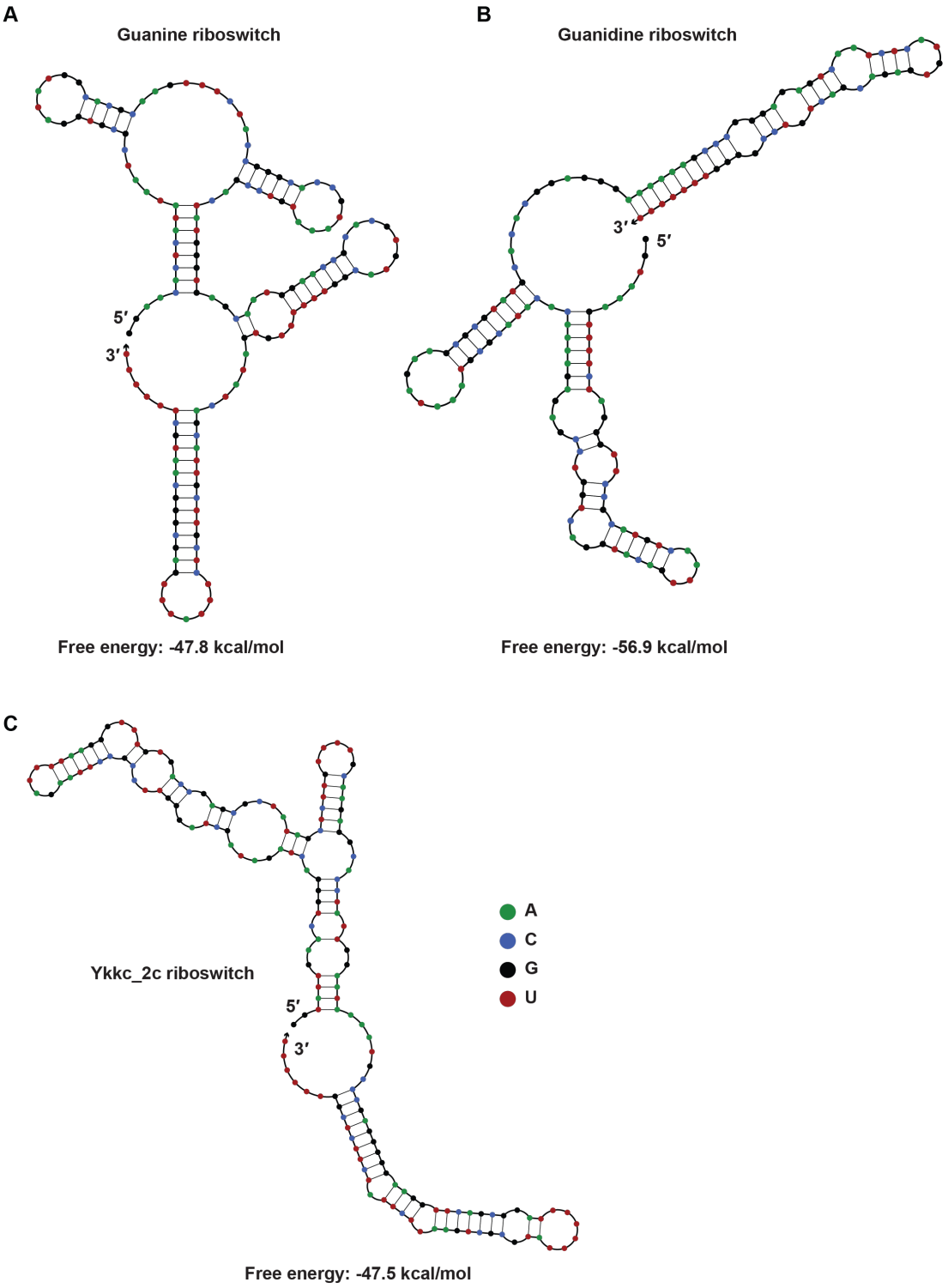

Supplementary Figure S1. Secondary structures and nucleotide content of riboswitches. Nucleic Acid Package (NUPACK) was used to predict secondary structure of (A) guanine riboswitch (151 nt), (B) guanidine riboswitch (148 nt), and (C) ykkc_2c nucleotide riboswitch (169 nt).

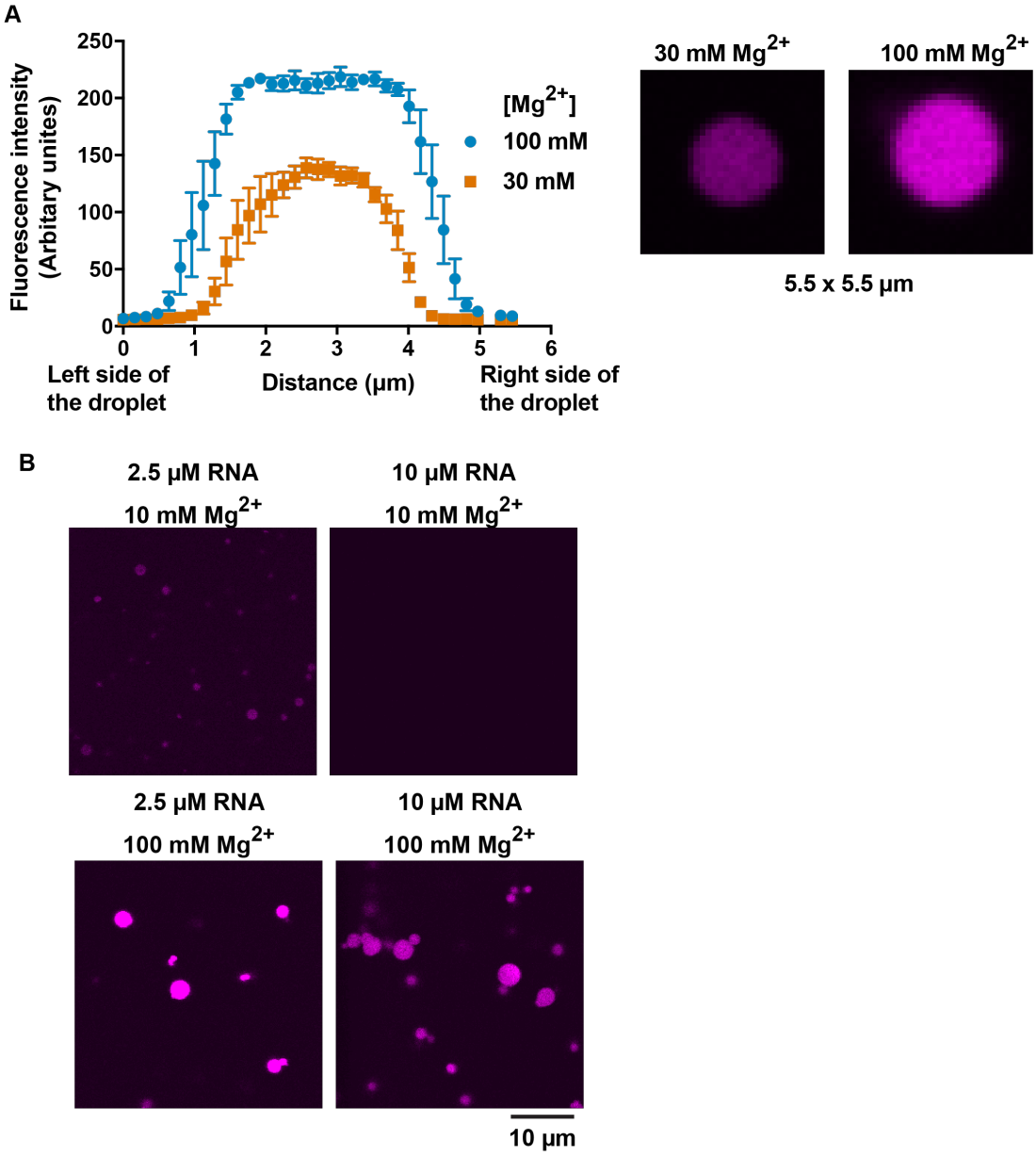

Supplementary Figure S2. Mg^{2+}-dependence of RNA condensation of the *Gdn* riboswitch. (A) (left) Fluorescence intensity across the droplets formed at 30 mM and 100 mM Mg^{2+} with 2.5 μM RNA. Field of view was visually inspected for the largest droplets for measurements (n=5). (right images) Representative image of a 5.5 x 5.5 μM field of view containing single droplets. (B) Condensation experiments performed using the indicated combination of Mg^{2+} and RNA concentrations.

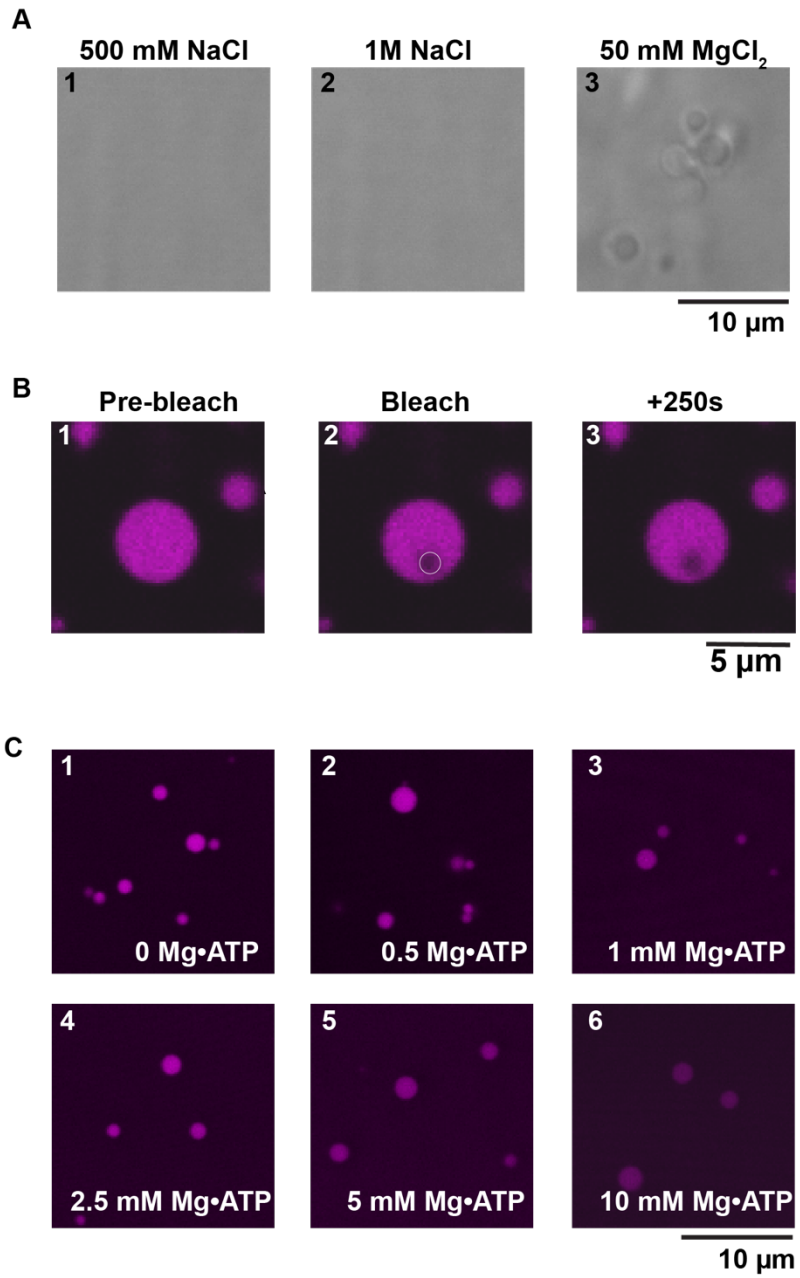

Supplementary Figure S3. Characterization of guanidine riboswitch condensates. (A) Condensates were formed as described in Figure 1, except Mg^{2+} was omitted for samples containing 500 mM and 1M NaCl. (B) For fluorescence recovery after photobleaching (FRAP) experiments, condensates formed using CF-647-labeled guanidine riboswitch as described in Fig 1. The indicated region of interest (ROI, white circle, ~1 µm) was bleached using 100% laser power (488 - 633 nm). Images were then collected every 10 sec. (C) To test whether RNA condensates are resistant to ATP, condensates were formed as described previously, except indicated amounts of Mg•ATP was added to the samples prior to renaturation.

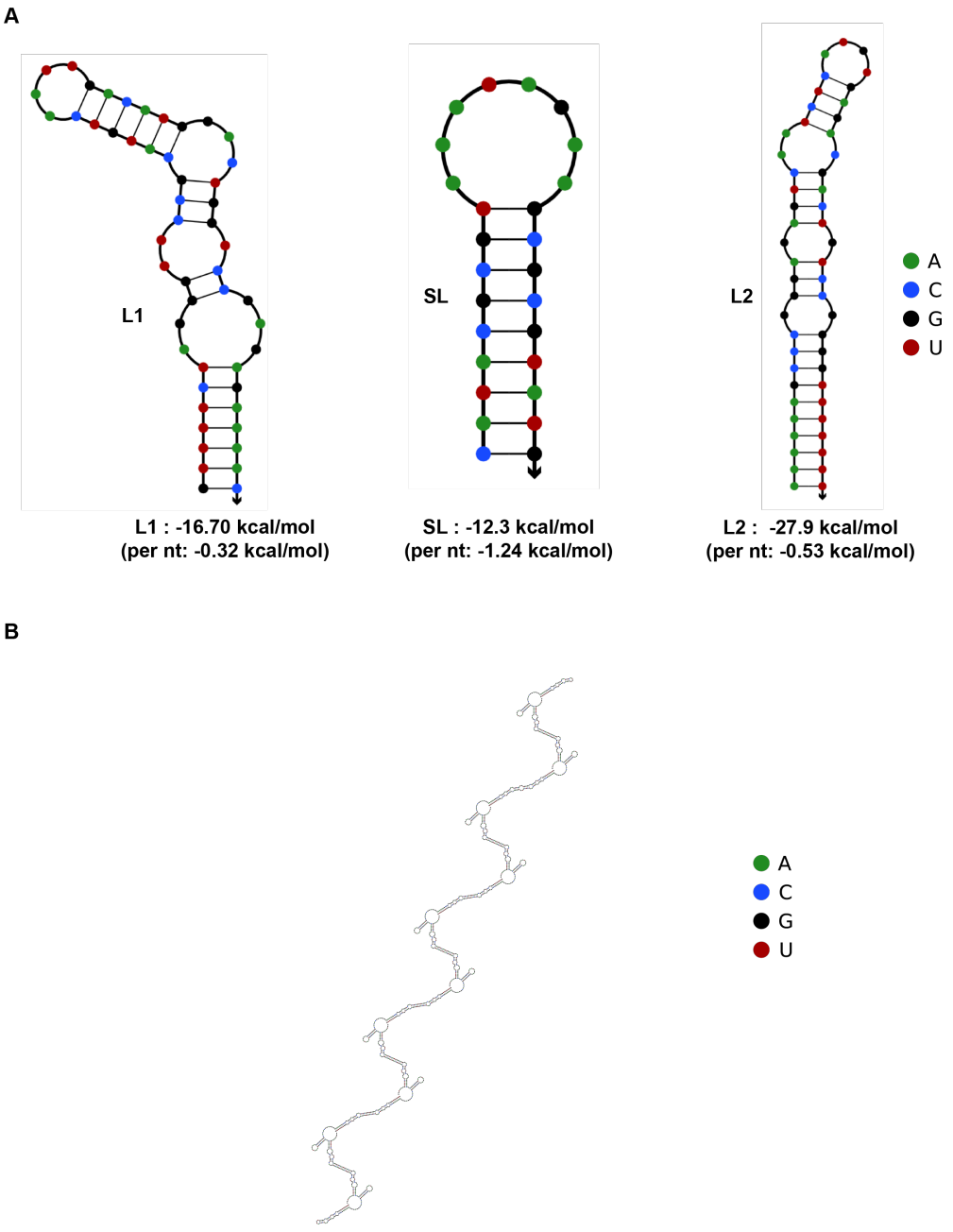

Supplementary Figure S4. Secondary structure of Gdn riboswitch RNA domains. (A) Secondary structures and the free energy of domains containing the L1 loop (left), SL region (middle), and L2 loop (right). Free energies associated with the structures are provided and free energy per nucleotide are shown in parenthesis. (B) Predicted multimerization of 10 monomers of Gdn riboswitch RNA.

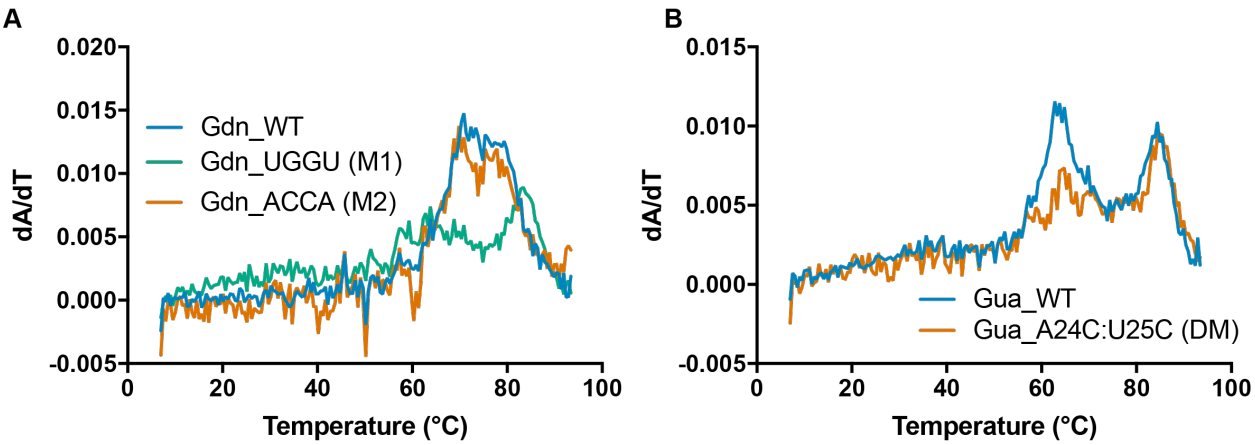

Supplementary Figure S5. UV-thermal melts of RNA. A) First derivative plots (260 nm) from thermal denaturation of WT and mutant guanidine riboswitches (B) Same as (A) but with mutant and WT guanine riboswitches.

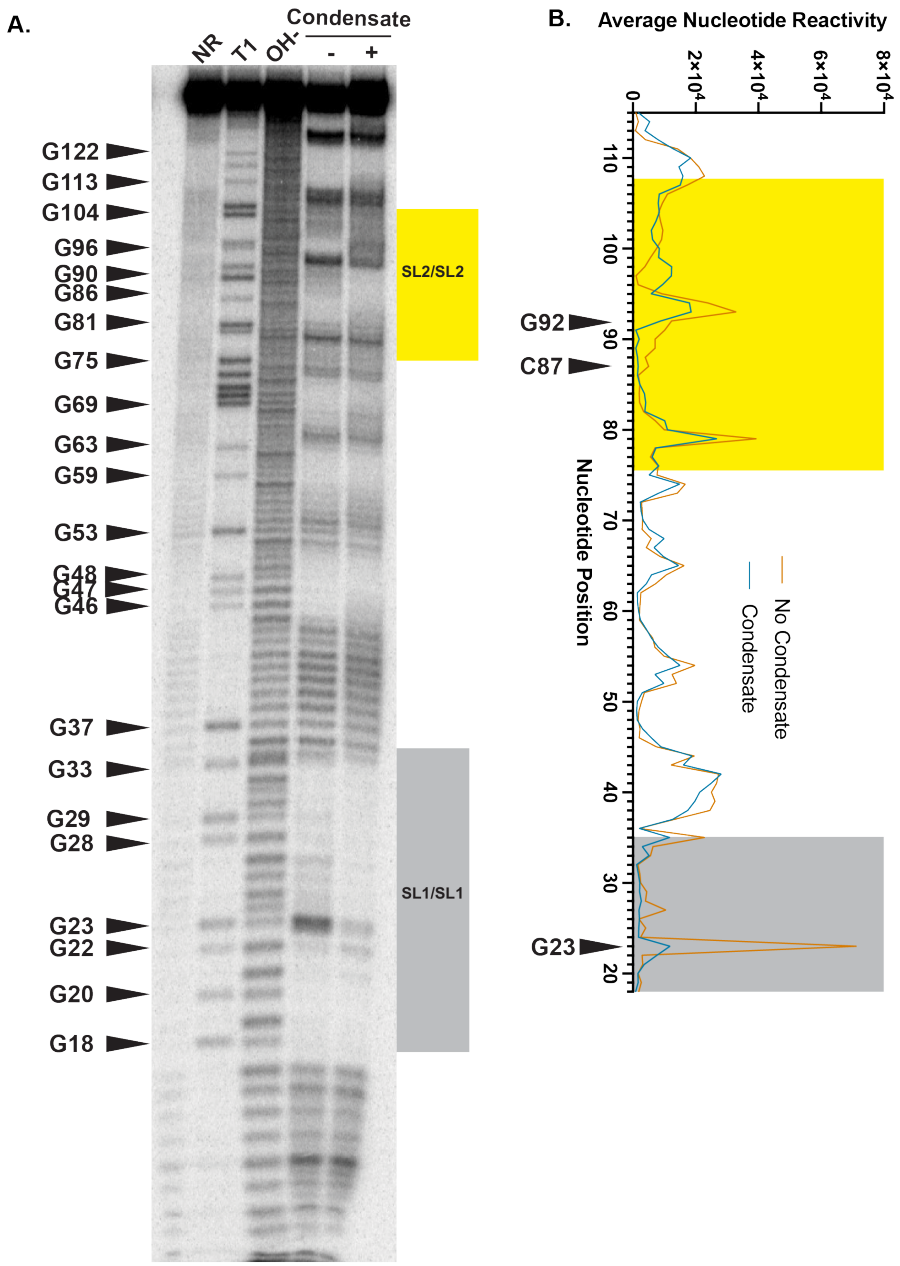

Supplementary Figure S6. In-line probing (ILP) analysis of Gua DM RNA condensate. (A) Gel image (10% Denaturing PAGE, 7M Urea) showing the cleavage pattern of 5′-end labeled RNA. Lane NR is trace (<3 nM) ^{32}P-labeled riboswitch after the renaturation step but without ILP. Lane T1 is treatment with RNase T1 to generate a ladder of Gs. Lane OH– is treatment with alkali to generate a ladder of all nucleotides. The condensate minus (–) lane contains trace ^{32}P-labeled riboswitch while the condensate plus (+) lane also contains trace ^{32}P-labeled riboswitch plus 5 μM unlabeled riboswitch to induce the formation of condensates. Loops in the monomer predicted to base pair during multimerization are indicated in gray (SL1/SL1) and yellow (SL2/SL2) (see Fig. 4 for reference.) (B) Plot of ILP reactivity in the no-condensate and condensate samples. Reactivities near the SL1/SL1 and SL2/SL2 regions are shaded in gray and yellow to color match with the gel. Data were quantitated by ImageQuant (Molecular Dynamics).

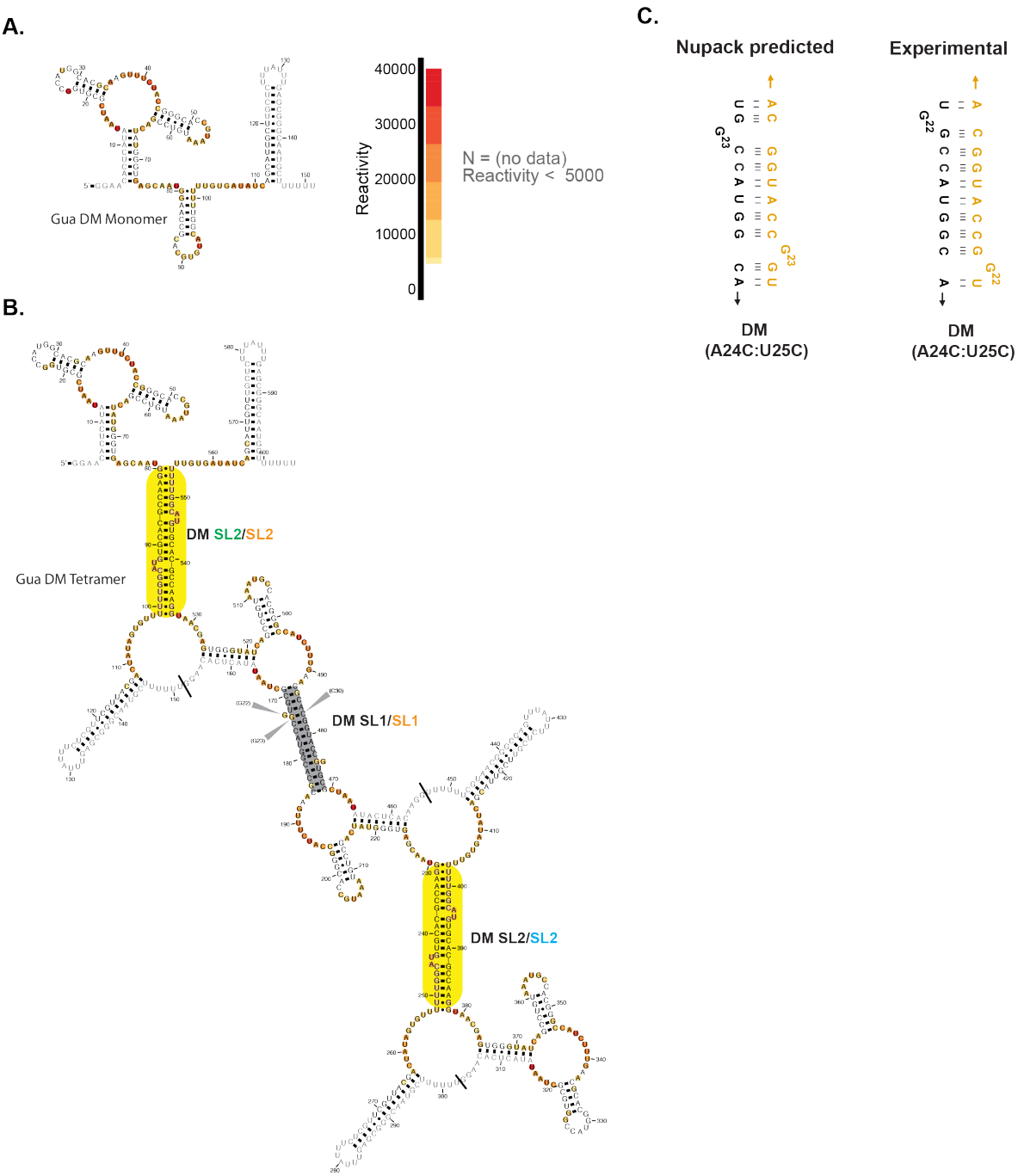

Supplementary Figure S7. Predicted structures of Gua DM monomer and tetramer with in-line probing (ILP) reactivity data overlaid. (A) Data for –condensate from Supplementary Figure S6 mapped to the secondary structure of monomer predicted by NUPACK. Two isolated base pairs predicted by NUPACK and shown in Supplementary Figure S1 are omitted since the data did not support them. (B) Data for +condensate from Supplementary Figure S6 mapped to the secondary structure of tetramer Gua DM RNA. Reactivities near the SL1/SL1 (shaded gray) and SL2/SL2 (shaded yellow) regions. Colors of monomers match with those in Fig. 4. (C) NUPACK-predicted model from Fig. 4B adjusted to show G23 as base-paired and G22 as unpaired, consistent with experiments. Average ILP reactivity from triplicate ILP reactions is shown in both panels.

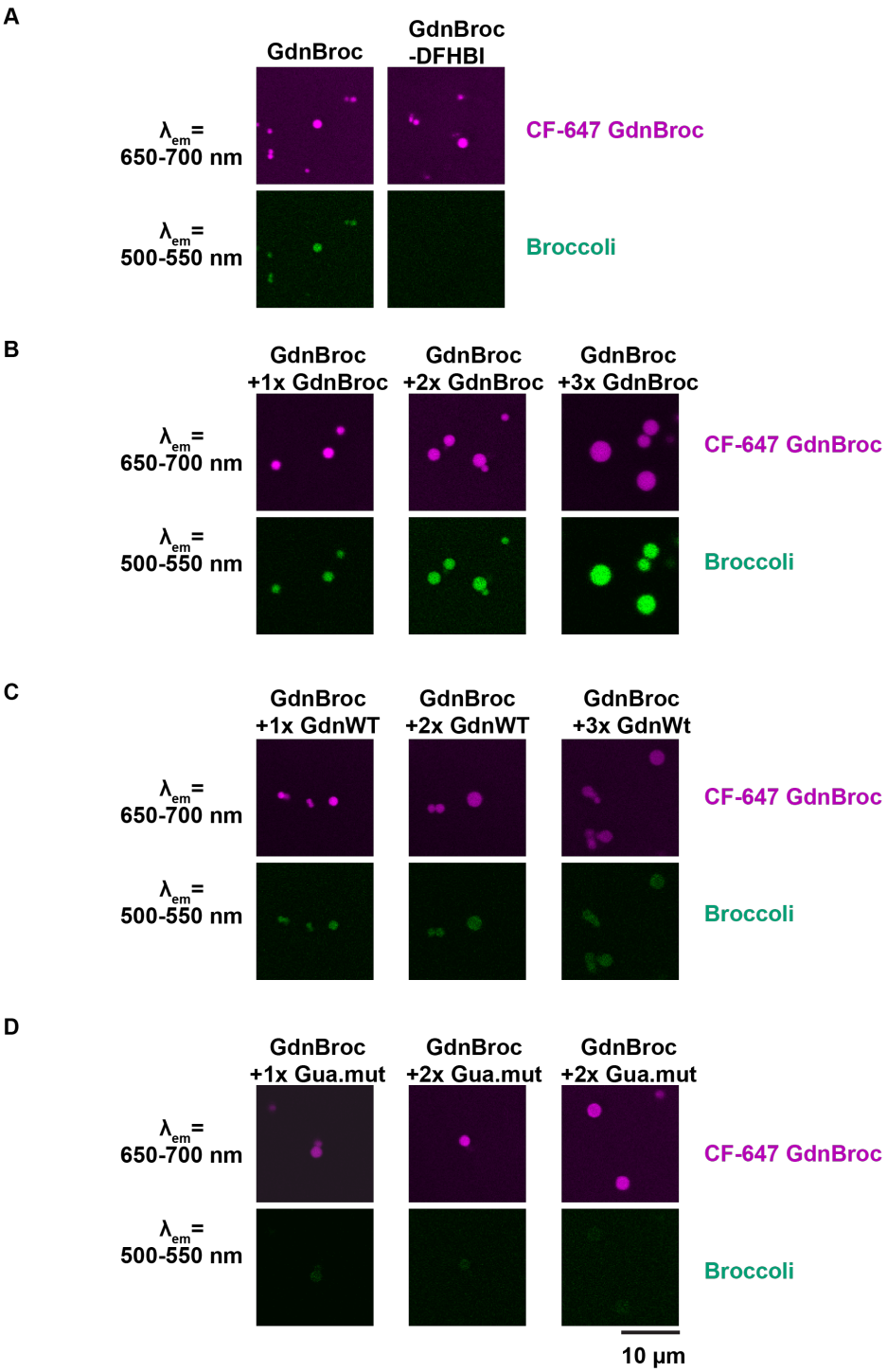

Supplementary Figure S8. Non-cognate RNAs result in misfold structure. (A) Condensates formed by broccoli-engrafted guanidine riboswitch (GdnBroc) show fluorescence signal in both CF 647 channel (magenta, top row) and broccoli channel (green, bottom row). CF 647 dye is tagged on the 3' of the RNA. (B) Condensates formed using CF-647 labeled GdnBroc RNA in the presence of increasing amounts of unlabeled GdnBroc. In (C) and (D) same experiments were performed with increasing amounts of unlabeled WT Gdn riboswitch (Gdn WT) or the U24C:A25C double mutant guanine riboswitch (Gua.mut). Plots provided in Fig. 6B are derived from these images (representative).

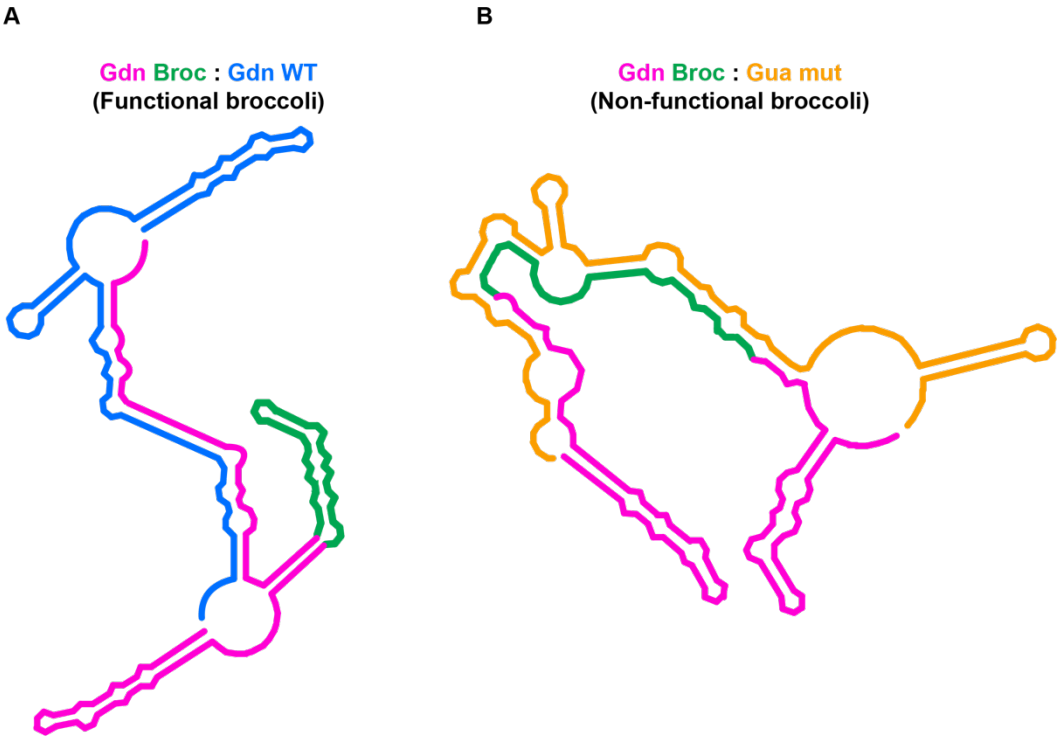

Supplementary Figure S9. Predicted structures of RNA heterodimers consisting of same or different scaffolds. (A) Dimerization of broccoli-engrafted guanidine riboswitch (GdnBroc, magenta + green) and WT guanidine riboswitch (Gdn WT, blue). (B) Dimerization of broccoli-engrafted guanidine riboswitch (GdnBroc, magenta + green) and U24C:A25C double mutant guanine riboswitch (Gua DM, orange). Note that broccoli aptamer is unfolded in panel B but not in panel A.